Journal of Materials Chemistry

Cite this: J. Mater. Chem., 2012, 22, 14155

www.rsc.org/materials

PAPER

A highly active and stable Pd–TiO_2/CDC–SiC catalyst for hydrogenation of 4-carboxybenzaldehyde

Yonghua Zhou,[ab] Xingyun Li,[a] Xiulian Pan*[a] and Xinhe Bao*[a]

Received 11th March 2012, Accepted 18th May 2012
DOI: 10.1039/c2jm31503c

Carbon has been widely used as a catalyst support and adsorbent in industry. However, it suffers from poor stability due to its limited mechanical strength, particularly under high pressures and temperatures. We report here a carbide derived carbon (CDC) layer on a porous SiC surface, which has the properties of high mechanical strength and is easy to shape. The CDC exhibits an amorphous structure and contains mainly mesopores with a BET surface area of 125 $m^2\ g^{-1}$. The CDC–SiC composite yields a comparable performance to coconut activated carbon (AC) as a catalyst support in the probe reaction hydrogenation of 4-carboxybenzaldehyde. The further introduction of TiO_2 nanoparticles enhances the activity and stability significantly because of the improved dispersion of Pd particles on CDC–SiC. The activity is 4 times higher than the Pd/AC catalyst. Pd–TiO_2/CDC–SiC shows great promise as an alternative to the current AC supported Pd catalyst for the crude terephthalic acid hydropurification industry.

1. Introduction

Activated carbon has been widely employed as the support of metal catalysts in chemical synthesis due to its advantages such as high surface area, resistance to acid and easy recovery of metals.[1–3] However, activated carbons from different sources can exhibit different compositions, morphologies and structures, which may lead to completely different performance. In addition, the low mechanical strength of activated carbon reduces its stability for high pressure reactions and the presence of a high microporosity can lead to mass transfer limitations, in *e.g.* fine chemical synthesis.[4] Therefore it is desirable to develop new support materials that can efficiently replace activated carbon.

For example, in catalytic hydropurification of crude terephthalic acid (CTA), coconut activated carbon (AC) gives the best performance and is currently used as a support for Pd. Terephthalic acid is an important intermediate for the manufacture of polyethylene terephthalate. Terephthalic acid is usually produced by the oxidation of *p*-xylene in liquid phase, which is often accompanied by impurities such as 4-carboxybenzaldehyde (4-CBA). 4-CBA can be removed *via* hydrogenation over a Pd/AC catalyst in a trickle bed reactor.[2] However, AC is easy to crush under the reaction conditions of relatively high pressure (7 MPa) and temperature (250 °C), which can lead to the loss of palladium and contamination of the product. Therefore, efforts have been made continuously to substitute the carbon support and a large amount of work has been focused on TiO_2.[5–8]

Recently SiC has attracted attention as a catalyst support because of its properties of high mechanical strength, easy shaping and high chemical stability.[9] For example, Ledoux and coworkers have developed a shape memory synthesis method for preparation of SiC and investigated the obtained SiC in reactions, *e.g.* selective oxidation of H_2S into S and direct oxidation of *n*-butane into maleic anhydride.[10,11] In order to overcome the limitation of its low surface area for practical applications, we intend to combine the advantages of carbon and SiC by using carbide derived carbon (CDC)–SiC composite as a support. CDC has been prepared by selectively etching the surface silica atoms using chlorine-containing gas.[12] The application of SiC in gas storage and micro-supercapacitors has been reported.[13,14] The important advantages of CDC over traditional activated porous carbons are its high purity, narrow pore size distribution, and the possibility to tune pore size.[15] However, it has not been explored yet in liquid phase reactions. We show here that the resulting CDC–SiC composite as the support for the Pd catalyst yields a comparable performance with respect to the commercial coconut activated carbon.

Inspired by previous studies,[16,17] we further introduced TiO_2 nanoparticles on the surface of the CDC–SiC composite. The resulting catalyst gives a significantly enhanced activity, as well as stability for the hydrogenation of 4-CBA due to the stabilization of the highly dispersed Pd nanoparticles.

[a]*State Key Laboratory of Catalysis, Dalian Institute of Chemical Physics, The Chinese Academy of Sciences, Zhongshan Road 457, Dalian, 116023, China. E-mail: panxl@dicp.ac.cn; xhbao@dicp.ac.cn; Fax: +86-411-84694447; Tel: +86-411-84686637*
[b]*Chemistry and Chemical Engineering College, Central South University, Lushannan Road 932, Changsha, 410083, China*

2. Experimental

2.1. Preparation of catalyst

β-SiC spheres with a diameter of 500–800 μm and a pore size of 20–100 nm were kindly supplied by SICAT company, France. The CDC layer over the SiC spheres was prepared by exposing SiC to a flowing gas mixture of Ar and CCl_4 vapor at atmospheric pressure at 840 °C. Subsequently, it was calcined in air at 400 °C for 2 h and then treated in 1 : 1 (volume ratio) nitric acid aqueous solution at 120 °C for 6 h. The resulting sample was denoted as CDC–SiC.

TiO_2 and Pd were loaded on CDC–SiC by a co-impregnation method. CDC–SiC was mixed with an isopropanol solution of tetrabutyl titanate and a toluene solution of $Pd(acac)_2$ under stirring at ambient temperature. After drying under ambient conditions, the sample was calcined in air at 400 °C for 3 h and then reduced in hydrogen at 250 °C for 2 h. The catalyst was denoted as Pd–TiO_2/CDC–SiC. The loadings of TiO_2 and Pd on the catalysts were 10% and 0.5% by weight, respectively.

For comparison, AC was purchased from Aladdin Company, China, which was currently used in industry. Pd was deposited on AC, CDC–SiC and SiC using the toluene solution of $Pd(acac)_2$ as the precursor. The resulting catalysts were denoted as Pd/AC, Pd/CDC–SiC and Pd/SiC, respectively. The Pd loadings in all catalysts were 0.5% by weight.

2.2. Characterization

The surface structure and morphology of the SiC spheres were examined with a QUANTA 200 FEG scanning electron microscope (SEM) at 20 kV. The Brunauer–Emmett–Teller (BET) surface areas were calculated from nitrogen physisorption data measured at 77 K with a Micromeretics ASAP 2400 apparatus. Raman spectroscopy was used to characterize the degree of disorder of the CDC layer on a LabRAM HR 800 apparatus (λ = 532 nm). X-Ray diffraction (XRD) was recorded using a Rigaku D/MAX-2500 instrument with Cu Kα radiation, a graphite mono-chromator with a scanning rate of 5° min^{-1}. The distribution of TiO_2 and Pd particles on the CDC–SiC composite was examined using high resolution transmission electron microscopy (TEM) on a TECNAI G^2 F30 operated at an acceleration voltage 300 kV.

2.3. Hydrogenation of 4-CBA

Hydrogenation of 4-CBA was conducted in batch mode in a stirred autoclave in the presence of 0.05 g catalyst, 0.20 g CBA and 80 g water, under a hydrogen pressure of 0.15 MPa and 90 °C. The concentration of 4-CBA was monitored every ten minutes, analyzed by HPLC.[18] The stability of the catalyst was tested by aging under a higher pressure and temperature than the usual reaction conditions, similar to a previous report.[18] 0.30 g of catalyst and 3.00 g of 4-CBA were kept in an autoclave at 200 °C with a hydrogen pressure of 1.5 MPa for 25 h. After aging, the catalysts were washed with ethanol and reduced in hydrogen at 250 °C before further activity tests under the same conditions.

3. Results and discussion

3.1. Characterization of CDC–SiC

The SEM images of β-SiC in Fig. 1 show that the SiC support is composed of small particles of several tens of nanometers and the pores are mainly sintered holes ranging from several nanometers to several hundreds of nanometers. This kind of SiC sphere is not suitable to act directly as a catalyst support because of the absence of meso- and micropores and functional groups.

After a layer of CDC forms on SiC under these conditions, the Raman spectra in Fig. 2 do not show the characteristic SiC peak at 750 cm^{-1} due to the shielding effect of the rather thick CDC layer, while an obvious D peak and G peak of carbon are observed. The presence of a strong D peak and a high intensity ratio of D peak to G peak (I_D/I_G) indicates that mainly amorphous carbon has been generated. In comparison, the I_D/I_G value for AC is 0.92, as shown in Fig. 2.

The adsorption isotherms and pore structures of the original SiC, the CDC–SiC composite and AC in Fig. 3 and Table 1 indicate that micropores and mesopores are generated in the CDC layer and the BET surface area increases from 34 m^2 g^{-1} to 125 m^2 g^{-1}. The pore volume of the micropores only occupies 5% of the total pore volume. In contrast, micropores occupy about 75% of the total pore volumes in the high BET surface area AC (as high as 1073 m^2 g^{-1}).

3.2. Characterization of Pd–TiO_2/CDC–SiC catalyst

After TiO_2 and Pd were loaded onto the surface of the CDC–SiC composite, the catalyst was characterized by XRD and high resolution TEM in order to identify the crystal phase, morphology and distribution of both TiO_2 and Pd. The XRD pattern of CDC–SiC in Fig. 4(a) shows the presence of carbon (2θ = 25.0°, 43.7°) and SiC (35.0°), which correspond to the 3C-SiC(111) crystal planes.[19] For the Pd/CDC–SiC catalyst, metallic Pd cannot be detected due to the rather low loading amount. When TiO_2 and Pd were loaded at the same time, the XRD pattern (Fig. 4(c)) shows that only the anatase phase of TiO_2 is present, which can be reflected at 25.3° (101), 37.8° (004), 48.0° (200), 53.9° (105) and 62.3° (204) as confirmed from JCPDS no. 2-1272. The fairly broad and weak diffraction peaks of anatase TiO_2 indicate the small crystalline size of TiO_2. At the same time, we do not observe diffraction of Pd for the Pd–TiO_2/CDC–SiC catalyst.

The high resolution TEM images of Pd–TiO_2/CDC–SiC in Fig. 5(a) and (b) show dispersion of TiO_2 particles on the surface of CDC-SiC. The lattice fringe of 0.36 nm corresponds to anatase

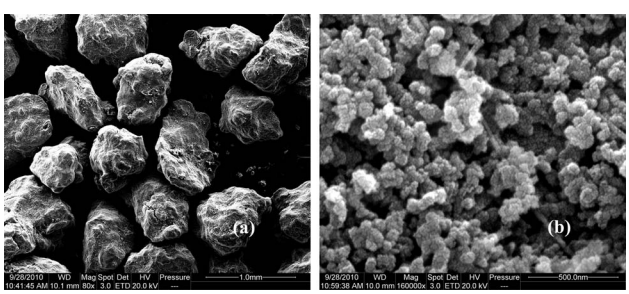

Fig. 1 SEM images of SiC support at different magnifications.

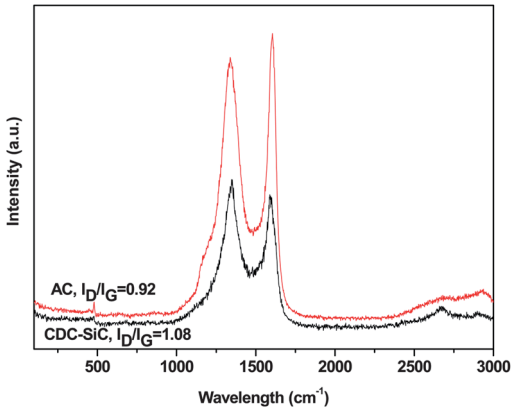

Fig. 2 Raman spectra of AC and CDC–SiC.

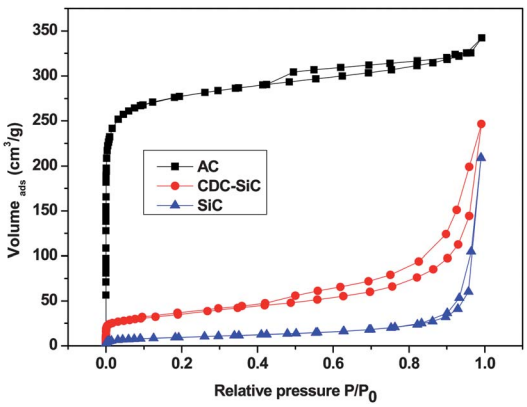

Fig. 3 Adsorption isotherms of AC, CDC–SiC and SiC.

(101) planes. Although EDX in Fig. 5(c) indicates the presence of Pd, particles with Pd lattice fringes are not observed. The EDX elemental mapping of Ti and Pd in Fig. 5(d) also supports our assumption that Pd and TiO_2 are homogeneously distributed. The TEM images in Fig. 6 shows that in the absence of TiO_2, larger Pd particles can be observed in the Pd/CDC–SiC catalyst, indicating worse dispersion of Pd.

3.3. Hydrogenation of 4-CBA

As reported previously, hydrogenation of 4-CBA is a first order reaction for 4-CBA.[18] Thus, the concentration of 4-CBA can be described by the following equation

$$\ln C_0/C_t = kt \quad (1)$$

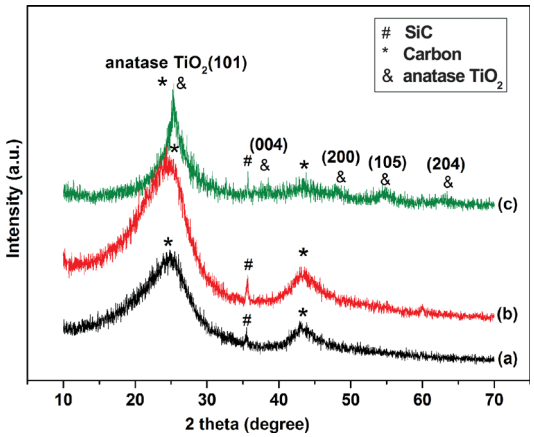

Fig. 4 XRD patterns of CDC–SiC (a), Pd/CDC–SiC (b) and Pd–TiO_2/CDC–SiC (c).

where C_0 is the initial concentration of 4-CBA, C_t is its instantaneous concentration at a given reaction time t, and k is the reaction rate constant. Since the reaction rate constant reflects the activity, we compare directly the rate constants over different catalysts.

Fig. 7 shows that using SiC directly as a support, the catalyst Pd/SiC has the lowest activity with a k value of 0.0001 min^{-1}. Pd/CDC–SiC gives $k = 0.0148$ min^{-1}, which is rather close to that of the Pd/AC catalyst ($k = 0.0152$ min^{-1}). In addition, the stability of the Pd/CDC–SiC catalyst is also comparable to Pd/AC, which can be reflected by the residual activity of 0.0031 min^{-1} and 0.0038 min^{-1} after aging. Thus, CDC–SiC shows promise as an alternative support for Pd.

To further enhance the activity and stability of the Pd/CDC–SiC catalyst in the 4-CBA hydrogenation reaction, we introduced TiO_2 nanoparticles onto the surface of CDC–SiC. As a result, the activity dramatically increased to 0.0591 min^{-1}, as shown in Fig. 8. This is almost 4 times that over Pd/AC and Pd/CDC–SiC (Fig. 7). Previous studies showed the dependence of the activity of 4-CBA hydrogenation on the Pd particle size.[20–22] Smaller particles with a higher dispersion lead to a higher activity. Our XRD, high resolution TEM and HAADF characterizations indicate highly dispersed TiO_2 particles on the CDC–SiC composite, which could improve the dispersion of Pd. The improved dispersion and reduced particle size of the Pt–Ru particles has been reported because of the presence of TiO_2 on the carbon support, which benefited methanol oxidation.[16] Zhao *et al.*[17] also observed that the addition of TiO_2 in a Pd/SiO_2 catalyst could reduce the size of the Pd particles significantly, which showed a higher ethylene yield in acetylene hydrogenation.

Table 1 Comparison of surface area and pore structure of AC, CDC–SiC and SiC[a]

	S_B (m^2 g^{-1})	S_m (m^2 g^{-1})	V_t (cm^3 g^{-1})	V_m (cm^3 g^{-1})	d (nm)
AC	1073	982	0.530	0.397	1.97
CDC–SiC	125	39.3	0.382	0.019	12.2
SiC	34	2.6	0.324	0.001	38.0

[a] S_B: BET surface area; S_m: T-method micropore surface area; V_t: total pore volume at $P/P_0 = 0.99085$; V_m: T-method micropore volume; d: average pore size.

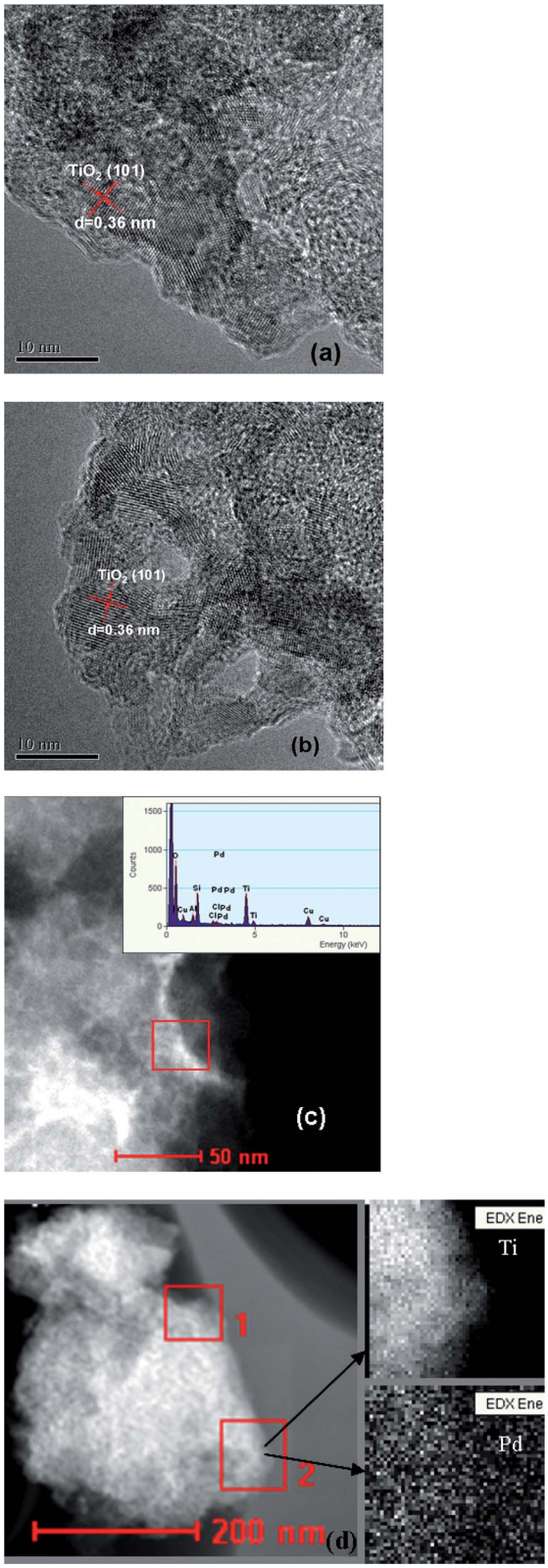

Fig. 5 High resolution TEM (a) and (b), HAADF image (c), and EDX elemental mapping of Ti and Pd in zone 2 with zone 1 as positioning for the Pd–TiO_2/CDC–SiC catalyst.

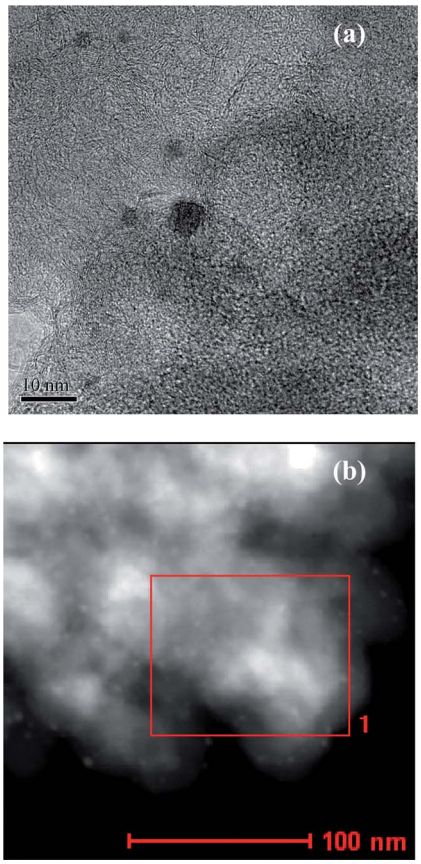

Fig. 6 High resolution TEM (a) and HAADF image (b) of Pd/CDC–SiC catalyst.

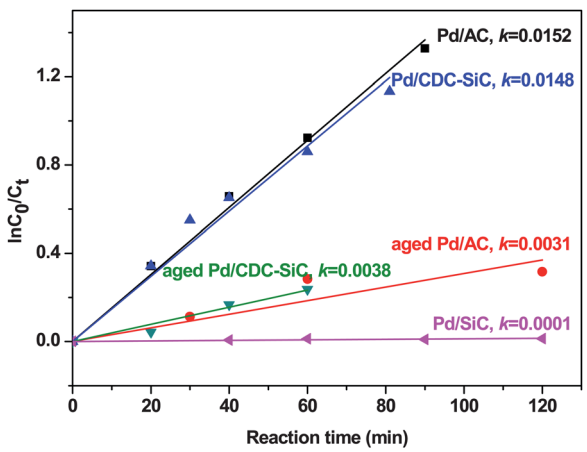

Fig. 7 Activities and stabilities of Pd/SiC, Pd/CDC–SiC and Pd/AC catalysts for the hydrogenation of 4-CBA. k is the reaction rate constant.

Fig. 8 also indicates that the activity of Pd–TiO_2/CDC–SiC decreases by less than a half from 0.0591 min^{-1} after aging. In the absence of TiO_2, the activity of the Pd/CDC–SiC catalyst drops by 73% from 0.0148 min^{-1} upon aging experiments. Therefore, in addition to an enhanced activity, the presence of TiO_2 improves the stability significantly with respect to the original Pd/CDC–SiC catalyst. The role of metal oxides in stabilizing noble metal particles on carbon supports has been reported previously. Kou

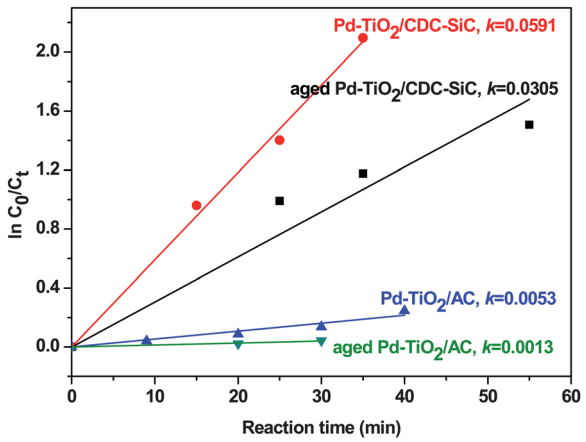

Fig. 8 Activities and stabilities of Pd–TiO_2/CDC–SiC and Pd–TiO_2/AC catalysts for hydrogenation of 4-CBA. k is the reaction rate constant.

et al.[23] deposited indium tin oxide (ITO) and Pt nanoparticles on graphene, forming a unique triple-junction structure (Pt–ITO–graphene), which exhibited greatly enhanced stability for oxygen reduction in PEM fuel cells. In our work, the presence of TiO_2 might have the same function and hence improves the stability of the Pd/CDC–SiC catalyst for hydrogenation of 4-CBA. In comparison, the introduction of TiO_2 to AC does not facilitate the reaction. Instead, Pd–TiO_2/AC (k = 0.0053 min^{-1}) shows a much lower activity than Pd/AC (Fig. 8). After aging, the activity decreases further (k = 0.0013 min^{-1}). In order to exclude the influence of oxygen functional groups which are often required for better dispersion of metal oxides, we treated AC with nitric acid (AC-n) and then deposited TiO_2 following the same procedure as Pd–TiO_2/AC. A similar k value (k = 0.006 min^{-1}) is obtained over Pd–TiO_2/AC-n as over Pd–TiO_2/AC. Comparison of the effects of TiO_2 on AC and SiC supported Pd catalysts implies that the pore structure is likely to play an important role because k is 0.001 min^{-1} for Pd/SiC and it increases to 0.012 min^{-1} for Pd–TiO_2/SiC. XPS indicates a decreased amount of surface Pd species in the presence of TiO_2, which is likely due to the entering of smaller Pd particles into the pores being promoted. These species are still accessible to reactants in the macropores of SiC and the mesoporous CDC layer, whereas they are not easy to reach for reactants in the micropores of AC although they are better dispersed. This is likely to be the reason for the different effects of TiO_2 on SiC, CDC–SiC and AC.

4. Conclusion

We report here a novel catalyst, Pd–TiO_2/CDC–SiC, consisting of highly dispersed Pd among TiO_2 nanoparticles on a support of a CDC layer on a porous SiC surface, which has the properties of high mechanical strength and is easy to shape. More importantly, Pd–TiO_2/CDC–SiC exhibits a 4 times higher activity and a much better stability than the conventional AC supported Pd catalyst for hydrogenation of 4-CBA.

Characterization of CDC–SiC composite shows that the CDC layer is dominated by mesopores although it is amorphous similar to AC and its BET surface area is 8 times less. The mesopores are beneficial for the inclusion of TiO_2 nanoparticles, which enhance the dispersion of Pd nanoparticles on CDC–SiC. In contrast, this does not work for coconut carbon because of its dominating micropores. Apart from the high activity and stability of Pd–TiO_2/CDC–SiC, the properties of high mechanical strength and the easy shaping of SiC render it promising for the industrial CTA hydropurification process which currently uses AC as the support for the Pd catalyst.

Acknowledgements

This work is supported by the National Science Foundation of China (no. 21006129, 11079005 and 21033009) and the Ministry of Science and Technology of China (2011CBA00503).

Notes and references

1 N. Krishnankutty and M. A. Vannice, *J. Catal.*, 1995, **155**, 312.
2 J. H. Bitter, *J. Mater. Chem.*, 2010, **20**, 7312.
3 F. B. Su, L. Lv, F. Y. Lee, T. Liu, A. I. Cooper and X. S. Zhao, *J. Am. Chem. Soc.*, 2007, **129**, 14213.
4 N. Pernicone, M. Cerboni, G. Prelazzi, F. Pinna and G. Fagherazzi, *Catal. Today*, 1998, **44**, 129.
5 H. Schroeder and R. L. Wittman, US 5 362 908, 1993.
6 M. Bankman, R. Brand and A. Freund, US 5 387 726, 1994.
7 T. M. Bartos and B. I. Rosen, US 5 616 792, 1996.
8 B. I. Rosen and T. M. Bartos, US 5 756 833, 1997.
9 P. O. Nubel, M. S. Haddad, J. J. Foster and R. L. Wittman, US 20080103333, 2008.
10 N. Keller, C. Pham-Huu and M. J. Ledoux, *Appl. Catal., A*, 2001, **217**, 205.
11 N. Keller, C. Pham-Huu, G. Ehret, V. Keller and M. J. Ledoux, *Carbon*, 2003, **41**, 2131.
12 G. Z. Cambaz, G. N. Yushin, Y. Gogotsi and V. G. Lutsenko, *Nano Lett.*, 2006, **6**, 548.
13 J. Chmiola, C. Largeot, P. L. Taberna, P. Simon and Y. Gogotsi, *Science*, 2010, **328**, 480.
14 S. H. Yeon, S. Osswald, Y. Gogotsi, J. P. Singer, J. M. Simmons, J. E. Fischer, M. A. Lillo-Rodenas and A. Linares-Solanod, *J. Power Sources*, 2009, **191**, 560.
15 S. Urbonaitea, L. Hälldahl and G. Svenssona, *Carbon*, 2008, **46**, 1942.
16 J. M. Chen, L. S. Sarma, C. H. Chen, M. Y. Cheng, S. C. Shih, G. R. Wang, D. G. Liu, J. F. Lee, M. T. Tang and B. J. Hwang, *J. Power Sources*, 2006, **159**, 29.
17 L. Y. Zhao, Z. W. Wei, M. Y. Zhu and B. Dai, *J. Ind. Eng. Chem.*, 2011, **18**, 45.
18 S. H. Jhung, A. V. Romanenko, K. H. Lee, Y. S. Park, E. M. Moroz and V. A. Likholobov, *Appl. Catal., A*, 2002, **225**, 131.
19 M. J. Ledoux and C. Pham-Huu, *CATTECH*, 2001, **5**, 226.
20 F. Menegazzo, T. Fantinel, M. Signoretto and F. Pinna, *Catal. Commun.*, 2007, **8**, 876.
21 K. T. Li, M. H. Hsu and I. Wang, *Catal. Commun.*, 2008, **9**, 2257.
22 R. Pellegrini, G. Agostini, E. Groppo, A. Piovano, G. Leofanti and C. Lamberti, *J. Catal.*, 2011, **280**, 150.
23 R. Kou, Y. Y. Shao, D. H. Mei, Z. M. Nie, D. H. Wang, C. M. Wang, V. V. Viswanathan, S. Park, I. A. Aksay, Y. H. Lin, Y. Wang and J. Liu, *J. Am. Chem. Soc.*, 2011, **133**, 2541.